High Performance Piezo-phototronic Devices Based on Intersubband Transition of Wurtzite Quantum Well

Minjiang Dan[1], Gongwei Hu[1], Jiaheng Nie[1], Lijie Li[2,*] and Yan Zhang[1,3,4,*]

[1] School of Physics, University of Electronic Science and Technology of China, Chengdu 610054, China

[2] College of Engineering, Swansea University, Swansea, SA1 8EN, UK

[3] Beijing Institute of Nanoenergy and Nanosystems, Chinese Academy of Sciences; Beijing 100083, China

[4] College of Nanoscience and Technology, University of Chinese Academy of Sciences, Beijing 100049, China

*To whom correspondence should be addressed, E-mail: zhangyan@uestc.edu.cn and L.Li@swansea.ac.uk

Abstract

III-nitride semiconductors play much more important roles in the areas of modern photoelectric applications, whereas strong polarization in their heterostructures is always a challenge to restrict the efficiency and performance of photoelectric devices. In this study, piezo-phototronic effect on near-infrared intersubband absorption is explored based on polar GaN/AlN quantum wells. The results show that externally applied pressure leads to the redshift of absorption wavelength by reducing polarization field of the quantum well. The sensitivity to estimate pressure-dependent intersubband absorption wavelength is almost two orders of magnitude higher than interband photoelectric devices. Additionally, such sensitivity is further enhanced by 2.6 times at 20 GPa as a result of piezo-phototronic effect. This study paves avenue for designing high performance near-infrared piezo-phototronic devices based on intersubband transition.

Keywords: Piezo-phototronic effect, GaN/AlN quantum well, intersubband transition, near-infrared absorption.

I. Introduction

Piezo-phototronics has acquired numerous research interests based on the coupled properties of piezoelectric, semiconductor and photoexcitation [1-3]. Polarization at junction or contact of piezoelectric semiconductors can be used for controlling carrier generation, transport and recombination [4, 5]. A variety of high performance devices have been developed, such as piezo-phototronic solar cells [6], LEDs [7] and pressure sensors [8]. InGaN/GaN quantum well array [9] and ZnO nanowire array [10] were utilized to achieve high-resolution distributed pressure imaging.

Pressure sensors converting external pressure stimulus into optical or electronic signals have found increasing applications in flexible electronics [11, 12], energy harvesting [13, 14] and human-computer interaction [15, 16]. Optical pressure sensors can extract the pressure values through wavelength shift under externally applied pressure. The interband transitions between conduction electrons and valence holes [17, 18] are typical in conventional InGaN/GaN quantum wells with sensitivity 0.002 GPa^{-1} at wavelength 0.441 μm [19]. InGaN quantum dot had a higher pressure sensitivity of 0.015 GPa^{-1} at wavelength 0.414 μm [20]. Intersubband transition is widely used in optoelectronic devices for infrared and terahertz applications [21, 22]. The infrared absorption wavelength ranges from 1.75 to 4.2 μm for GaN/AlGaN quantum wells [23]. Terahertz can be obtained by the intersubband electroluminescence of Si/SiGe quantum wells [24].

Polarization at GaN/AlGaN quantum wells was a well-proved approach to control the wavelength of intersubband transition [25, 26]. In this study, the pressure sensitivity of GaN/AlN quantum well has been calculated to reach up to 0.012 GPa^{-1} at 4.69 GPa, compared with 3.32×10^{-5} GPa^{-1} based on the interband transition [19]. The intersubband pressure sensitivity can be increased from 0.007 GPa^{-1} to 0.010 GPa^{-1} at 1.67 μm, indicating a 43% increase by the piezo-phototronic effect [27]. Here the absorption spectrum and wavelength are calculated by self-consistently solving the Schrödinger–Poisson equations. The results provide innovative guidance for high performance optical pressure sensors based on the piezo-phototronic effect.

II. Method and Model

Wurtzite GaN/AlN quantum well is comprised of two types of strong piezoelectric material, and only axial pressure acting on the materials are taken into account. Total polarizations can be calculated from $P_{piezo}^{b(w)} = P_{sp}^{b(w)} + e_{33}^{b(w)} S_{33}^{b(w)} + e_{13}^{b(w)} (S_{11}^{b(w)} + S_{22}^{b(w)})$, where the superscript $b(w)$ is the barrier (well) layer, e_{33} and e_{13} are piezoelectric coefficients, S_{11}, S_{22} and S_{33} are axial strains caused by the pressure and P_{sp} stands for the spontaneous polarization. Strain can be obtained from the strain-stress relationship $\boldsymbol{\sigma} = (\boldsymbol{C}) \bullet (\boldsymbol{s})$, where $\boldsymbol{C}$ is elastic constant, $\boldsymbol{\sigma}$ and $\boldsymbol{s}$ are the applied pressure and induced strain, respectively.

Except for pressure-produced strain, lattice-mismatched strain in barrier layer is also present and can be written as [28, 29] $S_{110}^{\mathrm{b}} = S_{220}^{b} = \frac{a_b - a_w}{a_w}$, $S_{330}^{b} = -\frac{2C_{13}}{C_{33}} s_{110}^{\mathrm{b}}$ and $S_{120}^{\mathrm{b}} = S_{230}^{b} = S_{310}^{b} = 0$, where a_b and a_b are lattice constants of barrier and well layers respectively, C_{13} and C_{33} are corresponding stiffness constants of AlN barrier layer. Here, we consider the quantum well pseudomorphically grown on GaN buffer layer, and thus GaN well layer has no lattice-mismatched strain. After obtaining polarization, we can solve built-in field in the quantum well [30] $E_b = \frac{(P_w - P_b) L_w}{\varepsilon_0 (L_b \varepsilon_{rw} + L_w \varepsilon_{rb})}$ and $E_b = -E_w \frac{L_w}{L_b}$, where electric field E_b, total polarization P_b, width L_b, and relative permittivity ε_{rb} are parameters of AlN barrier layer. Electric field E_w, total polarization P_w, width L_w, and relative permittivity ε_{rw} are parameters of GaN well layer. ε_0 denotes the vacuum permittivity.

The one-dimensional, effective-mass Schrödinger equation in quantum well system is solved from [31]

$$\left[-\frac{\hbar^2}{2m^*(z)} \frac{\mathrm{d}^2}{\mathrm{d}z^2} + V(z) \right] \psi(z) = E\psi(z) \tag{1}$$

where $\hbar$ is the reduced Plank's constant, m^* is the effective mass, V is the total potential energy in the conduction band, ψ is the electron wave function and E is the electron energy.

Electrical potential is given from one-dimensional Poisson equation [32]

$$\frac{\mathrm{d}}{\mathrm{dz}}\left[-\varepsilon_0\varepsilon_r(z)\frac{\mathrm{d}}{\mathrm{dz}}\phi(z)+P_{piezo}(z)\right]=q\left[N_{\mathrm{D}}(z)-n(z)\right] \tag{2}$$

where ε_r is the position-dependent relative permittivity, ϕ is the electrostatic potential which is part of the total potential energy V, P_{piezo} is the total piezoelectric charges, N_{D} is the ionized donor density and n is the free electron density. All results are obtained by mean of self-consistently solving Schrödinger and Poisson equations [33, 34]. Absorption coefficient of intersubband transition can be obtained as [29, 35]

$$\alpha_{\mathrm{abs}}=\frac{q^2\pi}{n_r c\varepsilon_0 m_0^2\omega d}\sum_{m,n}^{M,N}\int\frac{k_t dk_t}{2\pi}\int\frac{d\phi}{2\pi}\left|\mathrm{M}_{\mathrm{mn}}(k_t)\right|^2\frac{(f_m(k_t)-f_n(k_t))(\hbar\gamma/\pi)}{(\Delta E_{mn}-\hbar\omega)^2+(\hbar\gamma)^2} \tag{3}$$

where m_0 is the rest mass of electron in free space, n_r is the refractive index, c is the velocity of light, ω is the angular frequency of the incident light, d is the width of GaN well layer, M and N indicate the initial and final energy transition levels. $\mathrm{M}_{\mathrm{mn}}=\frac{m_z(E_m-E_n)}{i\hbar}\langle\varphi_m|z|\varphi_n\rangle$, where E_m and E_n are the mth and nth subband energy levels, respectively. $f(k_t)=[1+\exp((E_{m(n)}-E_F)/k_B T)]^{-1}$ is Fermi-Dirac function of conduction subband. $\hbar\gamma$ is the half linewidth of Lorentzian function and $\gamma=(0.1\mathrm{ps})^{-1}$ used here for simplicity. $\Delta E_{mn}=E_n-E_m$ is the transition energy.

Fig. 1(a) schematically shows the GaN/AlN quantum well structure, corresponding to potential profile of conduction band and wave functions under no externally applied pressure. The quantum well is formed by a 7 nm-thick GaN layer sandwiched between two 8 nm-thick AlN layers. Doping concentration of well and barrier layer are at the level of 10^{17} $\mathrm{cm^{-3}}$ and 10^{16} $\mathrm{cm^{-3}}$ and temperature is fixed at room temperature (300 K). The potential profile are inclined due to the presence of built-in field from spontaneous and piezoelectric polarization [36]. The arrow shows the intersubband transition from ground state to the first excited electronic state. Fig. 1(b) shows the case that quantum well is endured an externally applied pressure along [0001] direction. In this case, potential profile becomes flatter by pressure-induced piezoelectric polarization which is reversed to the built-in field, hence weakening it. The change of internal field in quantum well can effectively tune the subband energies and wave functions, thus control the intersubband transition of near-infrared photoelectric detection.

III. Results and discussion

Fig. 2(a) shows the pressure-dependent polarization field of well layer. As it can be seen, polarization field is weakened by pressure and has the magnitude of MV/cm. Such polarization field is so strong that the commonly used gate voltage cannot effectively control it. This is the reason why gate voltage is difficult to modulate photoelectric characteristics of polar quantum well. By contrast, polarization field in well layer is reduced by about 0.133 MV/cm per GPa. Fig. 2(b) shows intersubband absorption spectra under different external pressures. The absorption spectra are in the wavelength out of Restrahlen band of substrate materials (GaN, AlN and sapphire) [35, 37], hence it can be made available for designing photoelectric devices. Due to the light doping and selection rules, only intersubband transition from ground state to the first excited state and p-polarized light are mainly studied here. As we can see, absorption wavelength is increased with pressure, which is due to the quantum-confined Stark effect by the decrease of polarization field in GaN well layer [26, 38, 39]. Fig. 2(c) shows absorption wavelength as a function of pressure. Absorption wavelength increases monotonously from 1.66 μm to 2.24 μm when the pressure grows from 0 GPa to 20 GPa.

To estimate the ability of using pressure to control absorption wavelength, we calculate pressure sensitivity from [40]

$$S = \frac{\delta(\Delta\lambda / \lambda_0)}{\delta\sigma} = \frac{1}{\lambda_0} * \frac{\delta\lambda}{\delta\sigma} \tag{4}$$

where λ and λ_0 are the peak absorption wavelengths with and without external pressure, σ is the externally applied pressure. Fig. 2(d) shows the pressure sensitivity that is remarkably enhanced by pressure. At the pressure of 20 GPa, the sensitivity reaches to 0.026 GPa^{-1}, 2.6 times higher than that of no pressure. When a higher pressure is applied, the absorption spectrum moves into a longer wavelength and the device exhibits a better pressure sensitivity.

Fig. 3(a) shows absorption wavelength as a function of pressure in different quantum well widths. Absorption wavelength increases in near-infrared region with growing pressure for three quantum wells. Moreover, absorption wavelength becomes longer when the well width increases from 7 to 9 nm under a fixed barrier width of 8 nm. This is because of the weakened polarization field in well layer [41]. By contrast, increasing the barrier width from 8 to 10 nm leads to the decrease of absorption wavelength due to the enhanced polarization field [42].

Fig. 3(b) compares pressure sensitivity between the present work and previous experimental results [19, 43, 44]. It clearly shows that pressure sensitivity based on intersubband transition is much higher than those of interband transition. For those using the interband transition, pressure sensitivity has the value mostly at the level of 10^{-3}, whereas it is in level of 10^{-2} in this study. By increasing pressure from 0 to 19 GPa, its sensitivity rises from 7.66×10^{-4} GPa^{-1} to 0.025 GPa^{-1}. The improvement of absorption performance is attributed to the piezo-phototronic effect.

In order to globally study the influence of pressure and structure of quantum well, Fig. 4 shows the contour of intersubband absorption wavelength and its pressure sensitivity. Figs. 4(a, c) show the case under well width of 7 nm, and Figs. 4(b, d) show the case under barrier width of 8 nm. Fig. 4(a) shows that either increasing pressure (fixed barrier width) or decreasing barrier width (fixed pressure) can make absorption wavelength increased. In this situation, pressure sensitivity is enhanced by increasing pressure or lowing barrier width, as seen in Fig. 4(c). The variation of absorption wavelength and pressure sensitivity becomes reverse when well width is grown at a fixed barrier width, as shown in Figs. 4(b, d). This can be well understood since the dependence of polarization field of well layer on well and barrier width is exactly reverse from the periodic boundary condition $E_bL_b + E_wL_w = 0$ [30]. Even so, it has a common result that pressure can lead increased absorption wavelength and enhanced sensitivity.

Piezoelectric property of AlN barrier layer was already considered in this work. More calculations for one of dimension sets have been conducted for several scenarios in order to understand the impact of the polarization of the AlN layer (Fig. 5). Both AlN and GaN have strong piezoelectric properties. When the polarization of GaN and AlN layer are considered, absorption wavelength is red shifted due to the reduction of polarization field by pressure, as shown by the black dotted line in Fig. 5 and similar results in Figs. 2-4. When the piezoelectric property of AlN barrier layer is neglected in GaN/AlN quantum well, polarization field is enhanced by pressure leading to blue shift of the absorption wavelength, as shown by the blue line in Figure 5. It is seen from the blue line in Fig, 5, the absorption wavelength reduces from initially shifted 2.5 μm to 1.4 μm with the increase of pressure. The results match closely with previous findings in [45]. The red or blue shift phenomenon based on the intersubband transition mainly depends on the introduction of piezoelectric field [42]. The change of the absorption wavelength purely by pressure if not considering the polarization will be comparably very small, as seen from calculated results in Fig. 5 (red line).

IV. Conclusion

In summary, we have investigated the impact of piezo-phototronic effect on intersubband absorption in near-infrared wavelength in the GaN/AlN quantum well. On one hand, pressure sensitivity of intersubband absorption is much higher than those based on interband transition. On the other hand, external pressure can further enhance the intersubband sensitivity by the piezo-phototronic effect. Pressure sensitivity is also dependent on the width of barrier and well layer. This study provides a guidance for designing next generation high-sensitive near-infrared piezo-phototronic devices based on intersubband transition.

ACKNOWLEDGMENTS

The authors are thankful for the support from University of Electronic Science and Technology of China (Grant No.ZYGX2015KYQD063), and Engineering and Physical Sciences Research Council (grant no. EP/T019085/1).

Reference

1. *Wu, W. and Z.L. Wang, Piezotronics and piezo-phototronics for adaptive electronics and optoelectronics. Nature Reviews Materials, 2016.* ***1****(7).*
2. *Wang, Z.L., W. Wu, and C. Falconi, Piezotronics and piezo-phototronics with third-generation semiconductors. MRS Bulletin, 2018.* ***43****(12): p. 922-927.*
3. *Zhang, Y., et al., Theory of piezotronics and piezo-phototronics. MRS Bulletin, 2018.* ***43****(12): p. 928-935.*
4. *Zhang, Y. and Z.L. Wang, Theory of piezo-phototronics for light-emitting diodes. Adv Mater, 2012.* ***24****(34): p. 4712-8.*
5. *Zhang, Y., Y. Liu, and Z.L. Wang, Fundamental theory of piezotronics. Adv Mater, 2011.* ***23****(27): p. 3004-13.*
6. *Zhang, Y., Y. Yang, and Z.L. Wang, Piezo-phototronics effect on nano/microwire solar cells. Energy & Environmental Science, 2012.* ***5****(5).*
7. *Yang, Q., et al., Enhancing light emission of ZnO microwire-based diodes by piezo-phototronic effect. Nano Lett, 2011.* ***11****(9): p. 4012-7.*
8. *Sun, J., et al., Piezo-phototronic effect improved performance of n-ZnO nano-arrays/p-Cu2O film based pressure sensor synthesized on flexible Cu foil. Nano Energy, 2017.* ***32****: p. 96-104.*
9. *Peng, M., et al., High-resolution dynamic pressure sensor array based on piezo-phototronic effect tuned photoluminescence imaging. ACS Nano, 2015.* ***9****(3): p. 3143-50.*
10. *Pan, C., et al., High-resolution electroluminescent imaging of pressure distribution using a piezoelectric nanowire LED array. Nature Photonics, 2013. 7(9): p. 752-758.*
11. *Mannsfeld, S.C., et al., Highly sensitive flexible pressure sensors with microstructured rubber dielectric layers. Nat Mater, 2010.* ***9****(10): p. 859-64.*
12. *Someya, T., et al., A large-area, flexible pressure sensor matrix with organic field-effect transistors for artificial skin applications. Proc Natl Acad Sci U S A, 2004.* ***101****(27): p. 9966-70.*
13. *Wang, Z.L. and W. Wu, Nanotechnology-enabled energy harvesting for self-powered micro-/nanosystems. Angew Chem Int Ed Engl, 2012.* ***51****(47): p. 11700-21.*
14. *Yang, Y., et al., Human skin based triboelectric nanogenerators for harvesting biomechanical energy and as self-powered active tactile sensor system. ACS Nano, 2013. 7(10): p. 9213-22.*
15. *Jung, S., et al., Reverse-micelle-induced porous pressure-sensitive rubber for wearable human-machine interfaces. Adv Mater, 2014.* ***26****(28): p. 4825-30.*
16. *Silvera-Tawil, D., D. Rye, and M. Velonaki, Artificial skin and tactile sensing for socially interactive robots: A review. Robotics and Autonomous Systems, 2015.* ***63****: p. 230-243.*
17. *Mussener, J., et al., Bias-Controlled Optical Transitions in GaN/AlN Nanowire Heterostructures. ACS Nano, 2017.* ***11****(9): p. 8758-8767.*
18. *Spies, M., et al., Bias-Controlled Spectral Response in GaN/AlN Single-Nanowire Ultraviolet Photodetectors. Nano Lett, 2017.* ***17****(7): p. 4231-4239.*
19. *Jiang, J., et al., Direct lift-off and the piezo-phototronic study of InGaN/GaN heterostructure membrane. Nano Energy, 2019.* ***59****: p. 545-552.*
20. *Perlin, P., et al., Influence of pressure on the optical properties ofInxGa1−xNepilayers and quantum structures. Physical Review B, 2001.* ***64****(11).*

21. *Machhadani, H., et al., Intersubband absorption of cubic GaN/Al(Ga)N quantum wells in the near-infrared to terahertz spectral range. Physical Review B, 2011.* ***83****(7).*
22. *Machhadani, H., et al., GaN/AlGaN intersubband optoelectronic devices. New Journal of Physics, 2009.* ***11****(12).*
23. *Gmachl, C., H.M. Ng, and A.Y. Cho, Intersubband absorption in GaN/AlGaN multiple quantum wells in the wavelength range of λ∼1.75–4.2μm. Applied Physics Letters, 2000. 77(3): p. 334-336.*
24. *Lynch, S.A., et al., Intersubband electroluminescence from Si/SiGe cascade emitters at terahertz frequencies. Applied Physics Letters, 2002.* ***81****(9): p. 1543-1545.*
25. *Kladko, V., et al., Effect of strain-polarization fields on optical transitions in AlGaN/GaN multi-quantum well structures. Physica E: Low-dimensional Systems and Nanostructures, 2016.* ***76****: p. 140-145.*
26. *Łepkowski, S.P., et al., Piezoelectric field and its influence on the pressure behavior of the light emission from GaN/AlGaN strained quantum wells. Applied Physics Letters, 2001.* ***79****(10): p. 1483-1485.*
27. *Ha, S.H., H.Q. Liu, and J. Zhu, Temperature and pressure modulation on intersubband optical absorption in an Al Ga1-N/AlN core-shell nanowire. Superlattices and Microstructures, 2018.* ***123****: p. 183-188.*
28. *Grandjean, N., et al., Built-in electric-field effects in wurtzite AlGaN/GaN quantum wells. Journal of Applied Physics, 1999.* ***86****(7): p. 3714-3720.*
29. *Chuang, S.L., Optical gain of strained wurtzite GaN quantum-well lasers. IEEE Journal of Quantum Electronics, 1996.* ***32****(10): p. 1791-1800.*
30. *Ridley, B.K., W.J. Schaff, and L.F. Eastman, Theoretical model for polarization superlattices: Energy levels and intersubband transitions. Journal of Applied Physics, 2003.* ***94****(6): p. 3972-3978.*
31. *Harrison, P., Quantum wells, wires and dots. 2001: Wiley Online Library.*
32. *Sacconi, F., et al., Spontaneous and piezoelectric polarization effects on the output characteristics of AlGaN/GaN heterojunction modulation doped FETs. IEEE Transactions on Electron Devices, 2001.* ***48****(3): p. 450-457.*
33. *Saha, S. and J. Kumar, Fully self-consistent analysis of III-nitride quantum cascade structures. Journal of Computational Electronics, 2016.* ***15****(4): p. 1531-1540.*
34. *Tan, I.H., et al., A self-consistent solution of Schrödinger–Poisson equations using a nonuniform mesh. Journal of Applied Physics, 1990.* ***68****(8): p. 4071-4076.*
35. *Chih-Sheng, C., et al., Amplified spontaneous emission spectroscopy in strained quantum-well lasers. IEEE Journal of Selected Topics in Quantum Electronics, 1995.* ***1****(4): p. 1100-1107.*
36. *Reshchikov, M.A. and H. Morkoç, Luminescence properties of defects in GaN. Journal of Applied Physics, 2005.* ***97****(6).*
37. *Kucharski, R., et al., Transparency of Semi-Insulating, n-Type, and p-Type Ammonothermal GaN Substrates in the Near-Infrared, Mid-Infrared, and THz Spectral Range. Crystals, 2017. 7(7).*
38. *Leroux, M., et al., Quantum confined Stark effect due to built-in internal polarization fields in (Al,Ga)N/GaN quantum wells. Physical Review B, 1998.* ***58****(20): p. R13371-R13374.*
39. *Peng, L.H., C.W. Chuang, and L.H. Lou, Piezoelectric effects in the optical properties of strained InGaN quantum wells. Applied Physics Letters, 1999.* ***74****(6): p. 795-797.*

40. *Mannsfeld, S.C.B., et al., Highly sensitive flexible pressure sensors with microstructured rubber dielectric layers. Nature Materials, 2010.* ***9****(10): p. 859-864.*

41. *Friel, I., et al., Investigation of the design parameters of AlN/GaN multiple quantum wells grown by molecular beam epitaxy for intersubband absorption. Journal of Crystal Growth, 2005.* ***278****(1-4): p. 387-392.*

42. *Mii, Y.J., et al., Large Stark shifts of the local to global state intersubband transitions in step quantum wells. Applied Physics Letters, 1990.* ***56****(20): p. 1986-1988.*

43. *Huang, X., et al., Piezo-Phototronic Effect in a Quantum Well Structure. ACS Nano, 2016.* ***10****(5): p. 5145-52.*

44. *Kamińska, A., et al., Pressure-induced piezoelectric effects in near-lattice-matched GaN/AlInN quantum wells. Journal of Applied Physics, 2008.* ***104****(6).*

45. *Suzuki, N. and N. Iizuka, Effect of Polarization Field on Intersubband Transition in AlGaN/GaN Quantum Wells. Japanese Journal of Applied Physics, 1999.* ***38****(Part 2, No. 4A): p. L363-L365.*

Figure captions

Fig. 1 Schematic diagram of a single GaN/AlN QW and its corresponding potential profile of conduction band (a) without stress $\sigma = 0$ and (b) with stress $\sigma = 10$ GPa. The potential profile is calculated based on a QW with GaN and AlN width of 2 nm and 4 nm, respectively. e_1 and e_2 is wave function of ground state and first excited state. Intersubband transition occurs between e_1 and e_2 when a light with special wavelength is incident.

Fig. 2 (a) Polarization field in well layer as a function of external pressure. (b) Near-infrared absorption spectra under different pressures. (c) Absorption wavelength and (d) pressure sensitivity versus externally applied pressure.

Fig. 3 (a) Absorption wavelengths against pressure at different well and barrier widths. (b) Comparison of pressure sensitivity between present work and other studies.

Fig. 4 Contour plot of absorption wavelength versus applied pressure as well as (a) barrier layer width and (b) well layer width. Pressure sensitivity as a function of applied pressure as well as (c) barrier layer width and (d) well layer width. (a, c) and (b, d) are obtained under the fixed well width 7 nm and barrier width 8 nm, respectively.

Fig. 5 Absorption wavelengths versus pressure under different polarization conditions. Considering polarization for both GaN and AlN layers (black dotted line); only considering polarization for GaN layer (blue line); not considering polarization for both layers (red line).

Figures

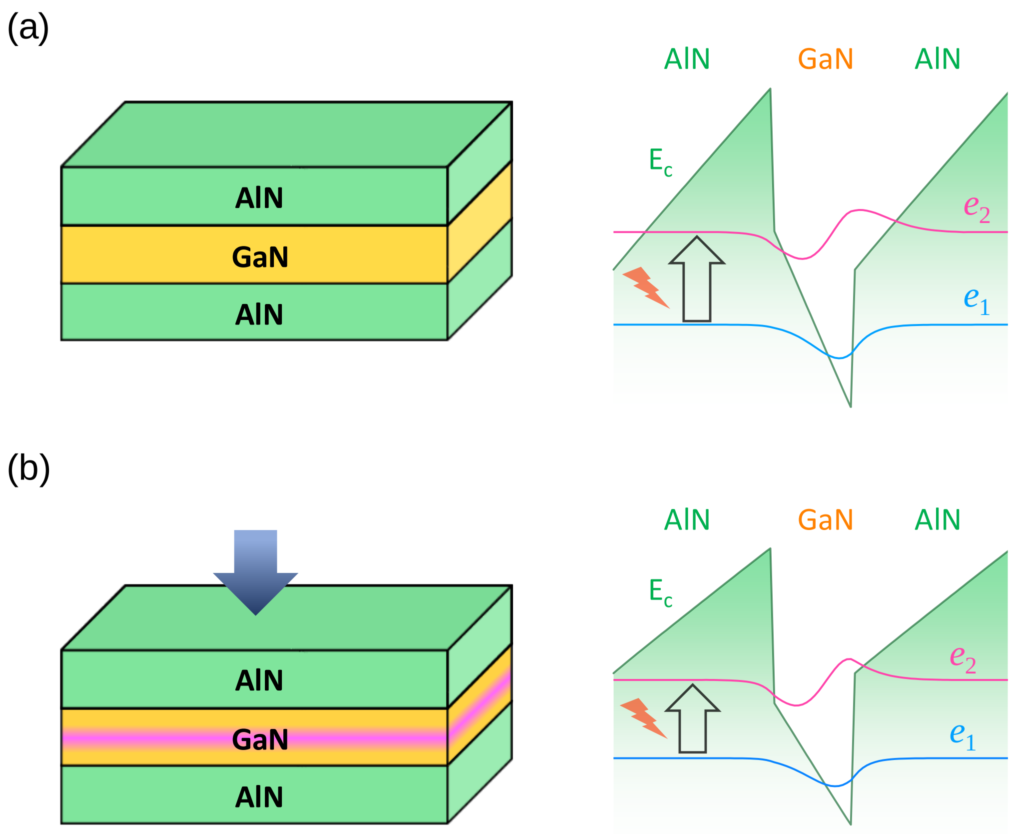

Figure 1

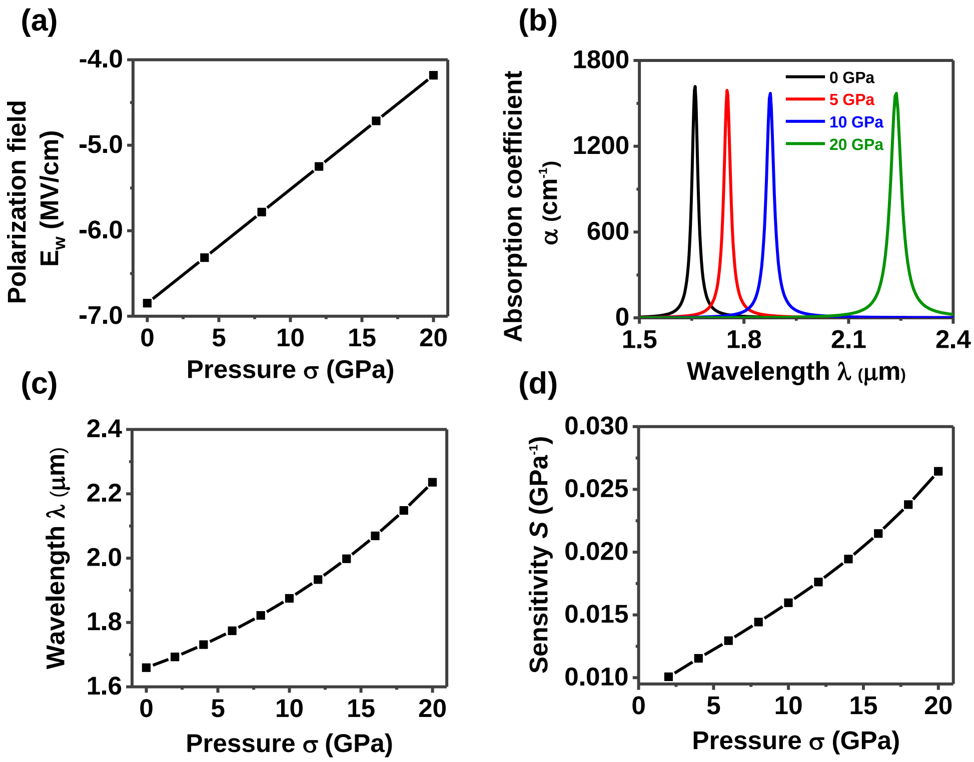

(a)
Polarization field
E_w (MV/cm)
-4.0
-5.0
-6.0
-7.0
0
5
10
15
20
Pressure σ (GPa)
(b)
Absorption coefficient
α (cm-1)
1800
1200
600
0
1.5
1.8
2.1
2.4
Wavelength λ (μm)
0 GPa
5 GPa
10 GPa
20 GPa
(c)
Wavelength λ (μm)
2.4
2.2
2.0
1.8
1.6
0
5
10
15
20
Pressure σ (GPa)
(d)
Sensitivity S (GPa-1)
0.030
0.025
0.020
0.015
0.010
0
5
10
15
20
Pressure σ (GPa)

Figure 2

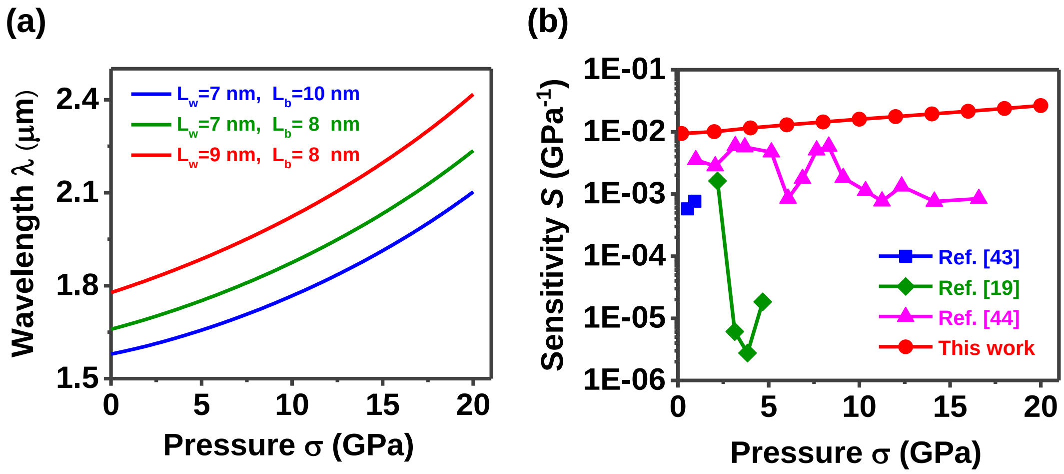
(a)
(b)
L_w=7 nm, L_b=10 nm
L_w=7 nm, L_b= 8 nm
L_w=9 nm, L_b= 8 nm
Wavelength λ (μm)
Pressure σ (GPa)
Sensitivity S (GPa^{-1})
Ref. [43]
Ref. [19]
Ref. [44]
This work

Figure 3

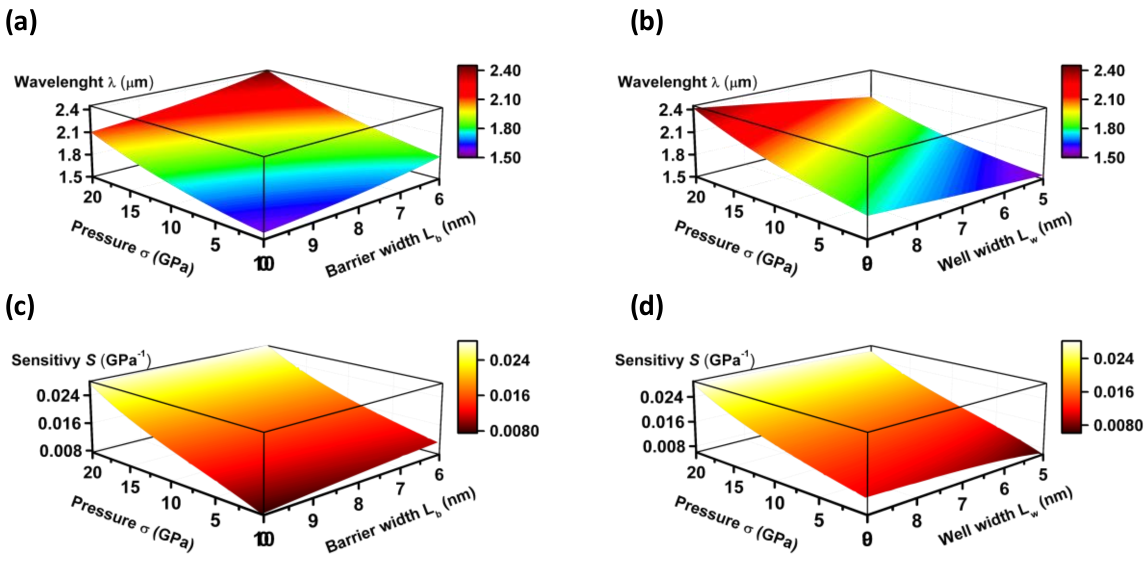

(a)
Wavelenght λ (μm)
2.4
2.1
1.8
1.5
2.40
2.10
1.80
1.50
20
15
10
5
Pressure σ (GPa)
Barrier width L_b (nm)
(b)
Wavelenght λ (μm)
Well width L_w (nm)
(c)
Sensitivy S (GPa^-1)
0.024
0.016
0.008
0.0080
(d)
Sensitivy S (GPa^-1)

Figure 4

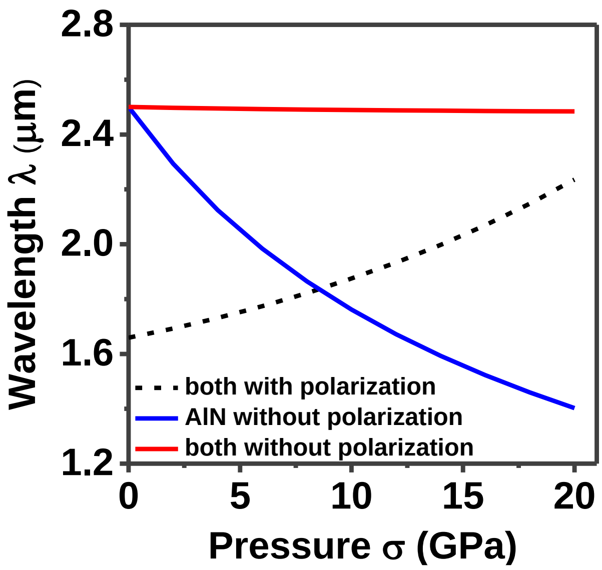

2.8
2.4
2.0
1.6
1.2
Wavelength λ (μm)
both with polarization
AlN without polarization
both without polarization
0
5
10
15
20
Pressure σ (GPa)

Figure 5

TOC Graphic

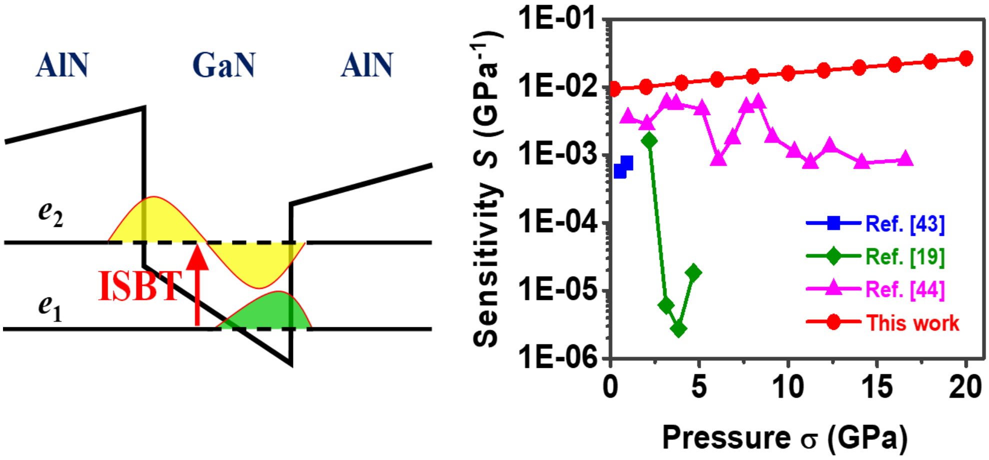

Piezo-phototronic effect on the intersubband absorption properties is investigated in GaN/AlN quantum well. Optical pressure sensitivity based on the intersubband transition is far higher than interband transition devices, which can be further improved by external applied strains.